Evaluation of the Effects of Tanezumab, a Monoclonal Antibody Against Nerve Growth Factor, on the Sympathetic Nervous System in Adult Cynomolgus Monkeys (*Macaca fascicularis*): A Stereologic, Histomorphologic, and Cardiofunctional Assessment

Patrice Belanger,[*,1] Paul Butler,[*] Mark Butt,[†] Siddhartha Bhatt,[‡]
Stephen Foote,[‡] David Shelton,[§] Mark Evans,[*] Rosalinda Arends,[‡]
Susan Hurst,[‡] Carlin Okerberg,[‡] Thomas Cummings,[‡] David Potter,[‡]
Jill Steidl-Nichols,[‡] and Mark Zorbas[*]

[*]Pfizer, Inc., San Diego, California 92121; [†]Tox Path Specialists, LLC, Frederick, Maryland 21701; [‡]Pfizer, Inc., Groton, Connecticut 06340; and [§]Pfizer, Inc., South San Francisco, California 94080

[1]To whom correspondence should be addressed at Pfizer Worldwide Research and Development, Drug Safety Research and Development, Pfizer, San Diego, CA 92121. Fax: (858) 678-8290. E-mail: patrice.belanger@pfizer.com.

ABSTRACT

Tanezumab, a humanized monoclonal antibody against nerve growth factor is in development for treatment of chronic pain. Three nonclinical studies assessed effects of clinically relevant and supratherapeutic doses of tanezumab on the sympathetic nervous system (SNS) of adult nonhuman primates. Study 1 evaluated potential effects of subcutaneous (SC) tanezumab (1.2 mg/kg every 8 weeks [Q8W]) on SNS in cynomolgus monkeys for 3 or 6 months and reversibility or persistence of any effects through a nondosing/recovery period. Study 2 evaluated whether neuronal cell death occurs shortly after a single SC tanezumab injection (1.2 mg/kg). Assessments for these two studies included evaluations of superior cervical and cervicothoracic ganglia for neuronal cell death and morphology. Study 3 evaluated effects of SC tanezumab (1.2 mg/kg Q8W and 30 mg/kg/week) over 6 months on sympathetic control of cardiovascular function. Tanezumab exposure was associated with stereologic changes in sympathetic ganglia, including smaller ganglion volume, and smaller average neuron size/area beginning at 2 weeks and reaching maximal levels by 1 month with no further progression through 6 months. These changes were not associated with clinical signs, completely reversed upon tanezumab withdrawal, and were not considered adverse. Tanezumab had no adverse effects on sympathetic control of cardiovascular function. These data support the conclusion that tanezumab administration for up to 6 months has no adverse effects on SNS morphology or function and does not cause neuronal cell death in adult nonhuman primates.

Key words: nerve growth factor; tanezumab; sympathetic ganglia; cynomolgus monkey.

Nerve growth factor (NGF) was first isolated and described based on its action on developing sympathetic and sensory neurons (Bueker, 1948). Inhibition of NGF produces profound loss of these neurons during development due to an increase in the magnitude of naturally occurring cell death, with primary sensory neurons being sensitive earlier in development than sympathetic neurons (Gorin and Johnson, 1979; Levi-Montalcini and Booker, 1960). In the adult, dependence of these neurons on NGF for survival has been addressed by in vitro and in vivo studies. Adult primary sensory neurons survive well in vitro in defined media without NGF, providing evidence they no longer require NGF for survival even though they respond to NGF with distinct morphologic and biochemical changes (Lindsay, 1988).

Data concerning NGF dependence of adult sympathetic neurons are more mixed. A number of in vivo rodent studies have examined the effects of NGF inhibition on the adult sympathetic nervous system (SNS) by treatment with anti-NGF antibodies. Although neuronal changes are not as immediate or extensive as seen in neonates, several studies reported an apparent loss of up to 75% of sympathetic neurons after chronic NGF-antibody exposure, and parallel studies showed a loss of biochemical parameters such as noradrenergic enzymes (Bjerre et al., 1975; Goedert et al., 1978; Gorin and Johnson, 1980; Johnson et al., 1982; Otten et al., 1979; Ruberti et al., 2000; Ruit et al., 1990). These data led to the conclusion that adult sympathetic neurons retain at least limited NGF dependence (Gorin and Johnson, 1980; Johnson et al., 1982; Otten et al., 1979; Ruberti et al., 2000; Ruit et al., 1990).

In apparent contradiction to these data, in vivo animal experiments that allowed recovery from NGF-antibody exposure demonstrated partial or complete recovery, suggesting the effects are not permanent and do not reflect actual neuron loss (Bjerre et al., 1975). Studies have reported a decrease in neurons (Ruit et al., 1990), presumed to be due to neuronal death, but no images of necrotic neurons accompany such studies, suggesting the reported decrease in counts may be due to under-recognition rather than actual loss of neurons. Providing further support to the concept that adult sympathetic neurons do not depend on NGF for survival are several in vitro studies in which neurons either allowed to "mature" in culture or taken from adult animals were shown to survive without NGF added to the media (Easton et al., 1997; Orike et al., 2001). Therefore, dependence of adult sympathetic neurons on NGF for survival remains an open question. This question has become more important recently due to the emergence of NGF inhibitors as potential new therapies for pain (Hefti et al., 2006; Mantyh et al., 2011), because it is critical to understanding potential side effects of chronic treatment with NGF inhibitors, such as tanezumab, fulranumab, and fasinumab (Hefti et al., 2006; Mantyh et al., 2011; Sanga et al., 2013; Tiseo et al., 2014).

We have reexamined this question in the nonhuman primate treated with tanezumab, a humanized IgG2Δa monoclonal antibody against NGF, by using a variety of techniques including electron microscopy. Our studies investigated effects of tanezumab on the SNS of cynomolgus monkeys via stereologic and histomorphologic assessment of sympathetic ganglia at 3 or 6 months (Study 1) and intensively over the first month (Study 2). The SNS has an important role in control of the cardiovascular system as well as in normal compensatory responses to postural changes critical to preventing orthostatic hypotension (OH) (Guyenet, 2006; Stewart, 2012). Therefore, a third study (Study 3) was conducted to examine effects of tanezumab on SNS function over 6 months by evaluating ambulatory cardiovascular parameters via telemetry and using a tilt paradigm to assess the risk of OH.

MATERIALS AND METHODS

Sexually mature male and/or female cynomolgus monkeys were used in all 3 studies. All procedures in study protocols were in compliance with applicable animal welfare acts and were approved by the local Institutional Animal Care and Use Committee. Animal care, including room, cage, and equipment sanitation, conformed to guidelines in the Guide for the Care and Use of Laboratory Animals (National Research Council, 1996).

Animal care and use. In Studies 1 and 2, sexually mature male and/or female cynomolgus monkeys were pair-housed in stainless steel cages with an animal of the same sex and treatment. Animals were offered Certified Primate Diet #2055C (Harlan Laboratories, Inc.) one or two times daily unless fasted for study procedures; water was provided ad libitum. In Study 3, animals were pair-housed except on days for assessment of ambulatory telemetry, when animals were separated the day before and returned to pair housing once assessment was completed. A standard diet of pelleted food (Certified Primate Diet 5K91, PMI Feeds) supplemented with vegetables and/or fruits was provided twice daily.

At initiation of dosing in Study 1, animals were 4–7 years old and body weights ranged from 5.6 to 10.5 kg for males and 2.8 to 5.4 kg for females. At initiation of dosing in Study 2, male animals were 4–8 years old and body weights ranged from 4.7 to 9.7 kg. For Study 3, animals were >2.5 years old and body weights ranged from 2.5 to 10.0 kg at initiation of dosing.

Tanezumab administration and study design. Tanezumab was manufactured and supplied by Pfizer Inc. (Puurs, Belgium) in a vehicle consisting of 10 mM histidine, 84 mg/ml trehalose, 0.1 mg/ml polysorbate 20, and 0.05 mg/ml ethylenediaminetetraacetic acid buffer, with a pH of 6.0. The dose volume for all dose groups was 3 ml/kg.

In Study 1, male and female cynomolgus monkeys were treated with subcutaneous (SC) tanezumab 1.2 mg/kg ($n = 33$) or 0 mg/kg (vehicle control, $n = 64$) every 8 weeks (Q8W) for up to 24 weeks (ie, up to 3 doses; Figure 1A). Animals were divided into 3 cohorts: Cohort 1 ($n = 12$ treated, 24 controls) was sacrificed after 3 months of dosing (2 doses); cohort 2 ($n = 11$ treated, 24 controls) was sacrificed after 6 months of dosing (3 doses); cohort 3 ($n = 10$ treated, 16 controls) was treated for 6 months and sacrificed following an 8-month (females) or 10-month (males) nondosing recovery period. The duration of the recovery period was such that the plasma tanezumab concentration for each animal was predicted to be below 6 ng/ml for at least 3 months prior to sacrifice. The dose and dosing regimen of 1.2 mg/kg/Q8W SC were predicted to result in exposure 5-fold higher than that seen in clinical trials based on the average concentration at steady-state (C_{ave}), third dose area under the concentration–time curve from hour 0 to hour 1344 ([AUC_{1344}]/8-week dosing interval), and a 9-fold margin based on the peak concentration (C_{max}), over the C_{ave} and C_{max} achieved with a clinical SC dose of 10 mg Q8W, while producing a pattern of tanezumab exposure as close to that observed in humans as possible.

In study 2, male cynomolgus monkeys were treated with a single administration of tanezumab SC at 0 mg/kg (vehicle control, $n = 24$) or 1.2 mg/kg ($n = 24$). Subsets of monkeys ($n = 6$ per treatment group) were sacrificed at 48 h, 1 week, 2 weeks, and 1-month postdose (Figure 1B).
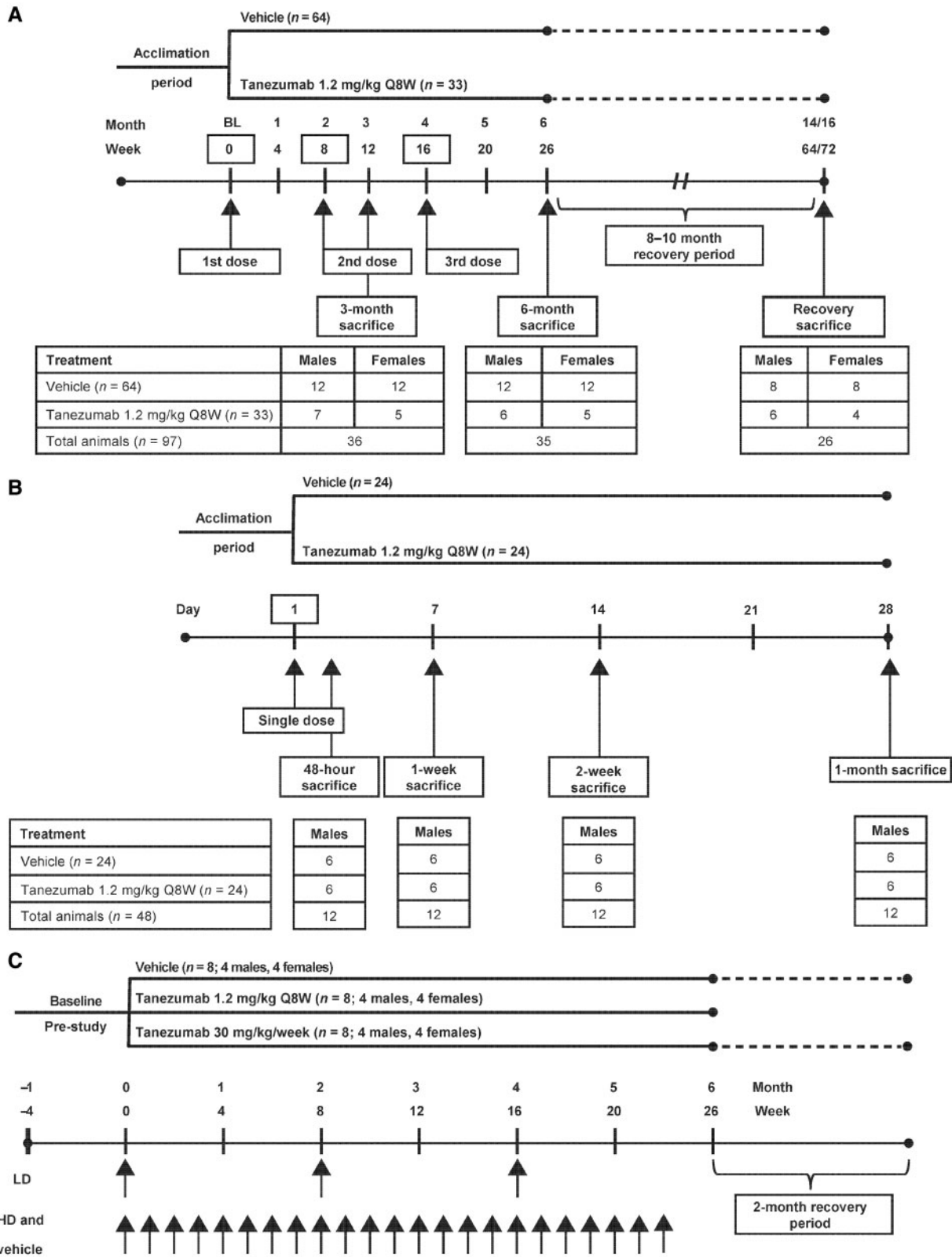
Figure 1. Study designs: A, study 1; B, study 2; C, study 3. Q8W, every 8 weeks; BL, baseline; HD, high dose; LD, low dose.

In study 3 (cardiovascular study), male and female cynomolgus monkeys (n = 8, [4/sex] per treatment group) were treated with tanezumab SC at 1.2 mg/kg/Q8W (3 doses) or 30 mg/kg/ week (23 doses) for ~6 months. A third group received vehicle treatment once weekly and served as controls (Figure 1C). At the end of the 6-month treatment period, animals in the

low-dose group were sacrificed, whereas animals in the vehicle and high-dose groups underwent a 2-month nondosing recovery phase and were then sacrificed (Figure 1C).

Toxicokinetic and anti-drug antibody analyses. Tanezumab concentration and anti-drug antibody (ADA) analyses were conducted at ICON Development Solutions (Whitesboro, NY). Toxicokinetic (TK) parameter calculations were conducted at Covance Laboratories (Madison, WI) and included C_{max}, time to peak concentration (T_{max}), C_{ave}, area under the concentration–time curve (AUC), and elimination half-life ($t_{1/2}$) when appropriate. Plasma concentrations of tanezumab were determined using a validated ELISA for detection and quantitation of tanezumab (Bowman et al., 2015; Zorbas et al., 2011). The lower limit of quantitation for tanezumab in monkey plasma for the bioanalytical assay was 100 ng/ml. Anti-drug antibody analysis of serum was conducted using an ELISA validated for the detection of anti-tanezumab antibodies (Bowman et al., 2015; Zorbas et al., 2011). Mouse anti-tanezumab IgG affinity-purified antibody was used as the positive control.

Tissue preparation. Tissues for morphology and stereology (studies 1 and 2 only) included the superior cervical ganglia (SCG) and the cervicothoracic ganglia (CTG) prepared as previously described (Butt et al., 2014). Briefly, at necropsy the monkeys were whole-body perfused with 4% methanol-free formaldehyde and the SCG and CTG were harvested, placed into cassettes, and stored in 4% methanol-free formaldehyde. The ganglia were embedded in paraffin and step-sectioned at 18 μm (study 1; Figure 2A) or a combination of 5 and 18 μm (study 2; Figure 2B). At 360-μm intervals throughout the entire ganglion, one 18-μm section was mounted to a slide, stained with H&E (a standard cell stain used for the majority of preclinical safety studies) and used for morphology and stereology investigations. In addition, at 6 systematic random levels throughout the ganglion, 1 slide was stained with NeuroApop/TUNEL (terminal deoxynucleotidyl transferase dUTP nick end labeling); a method for detecting DNA fragmentation by labeling the 3′-OH termini in the double-strand DNA breaks generated in the course of apoptosis (FD NeuroApop Kit, FD Neurotechnologies, Inc., Columbia, MD), another slide was stained with fluoro-jade B (FJB, a stain allowing for sensitive and selective identification of necrotic neurons; Histo-Chem, Inc., Jefferson, AR) to detect necrosis (Schmued and Hopkins, 2000), and a third slide was stained with H&E and used for morphology (study 2 only; Figure 2B). Neuronal cell death and morphology evaluations were performed on the sympathetic ganglia in both study 1 (SCG and CTG) and study 2 (SCG; Table 1). In addition, the CTG from all monkeys in study 2 was evaluated for morphology and neuronal cell death by transmission electron microscopy (TEM) at all time points (48-h, 1 week, 2 weeks, and 1-month postdose; Table 1).

Neurohistopathology. Neurohistopathology assessments were performed at Tox Path Specialists, LLC (Frederick, MD). Assessment of neuronal cell death and morphology included studies optimized for the detection of neuronal cell necrosis/apoptosis via a comprehensive light microscopic morphologic evaluation using: H&E (Figure 4), FJB (Supplementary Figure 1), and FD NeuroApop/TUNEL (Supplementary Figure 2).

Stereologic evaluations. Stereologic assessments were performed at Tox Path Specialists, LLC using Stereologer software (Stereology Resource Center, Chester, MD) as previously described (Butt et al., 2014). Ganglion volume was determined based on the Cavalieri method (Gundersen et al., 1999). The average neuron size/area was determined from the average cross-section area (calculated from the average radius determined using the nucleator method) of each counted neuron. The total neuron count was estimated from the number of neurons counted in a subset of each of the ganglion tissue sections examined, using the optical fractionator method (Mouton, 2002). For both studies, the coefficient of error (CE, estimated precision of the population size when using the optical fractionator) (Gundersen et al., 1999) for total neuron count was 0.0541–0.0990, while the CE for ganglion volume and average neuron size/area was ≤0.0231.
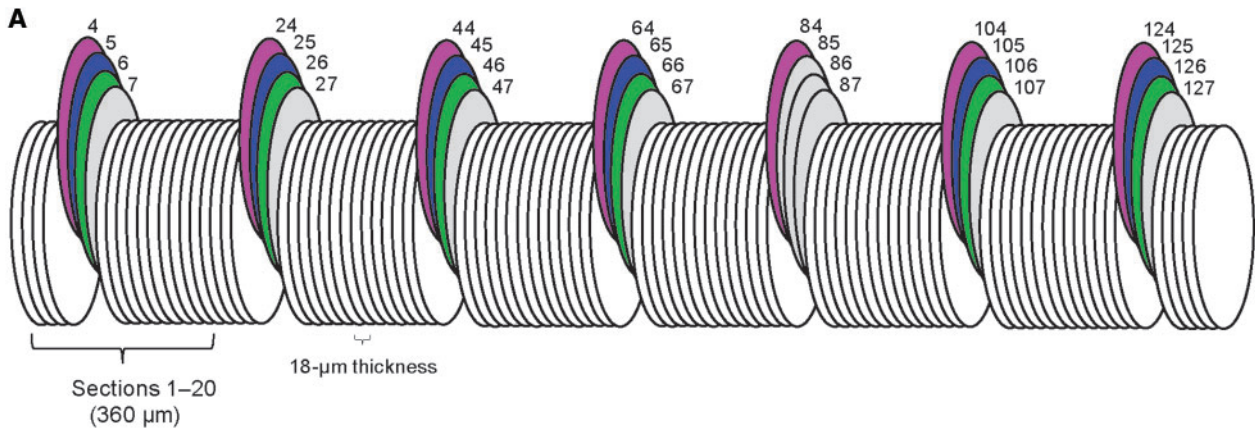
Transmission electron microscopy (study 2). Transmission electron microscopy evaluations were performed at Pfizer Global Research and Development (Groton, CT) by the study pathologist (blinded to treatment but not to study time points). Resin-embedded, toluidine blue-stained, 0.5-μm sections (1–3 sections per ganglion) from the middle of the CTG were produced for light microscopic (morphologic) evaluation. From the 0.5-μm sections, ultra-thin (75–90 nm) sections were cut, mounted on 200 mesh copper-palladium grids, counter-stained with uranyl acetate and lead citrate, and examined using TEM. Images of ganglia were viewed at magnifications suitable to discern ultrastructural morphology and identify the various cell types including neurons and neuronal appendages, satellite glial cells, Schwann cells, and interstitial components.

Telemetry (study 3). A total of 24 monkeys were fitted with radiotelemetry devices (TL11M2-D70-PCT, Data Sciences International, St. Paul, MN) for transmission of arterial blood pressure (BP), activity, and body temperature data. A gel-filled pressure catheter was placed into the femoral artery and advanced to lie just caudal to the renal arteries within the descending aorta. The transmitter body was placed within an intramuscular pocket created within the flank of the monkey.

Ambulatory cardiovascular parameters (BP, heart rate [HR], body temperature and activity) were assessed for ~24 h using telemetry in unrestrained, conscious animals 2 times prestudy (baseline) and monthly throughout the treatment phase (Figure 1C).

Tilt assessment (study 3). The radiotelemetry device-fitted monkeys were also evaluated using a validated tilt paradigm to investigate the risk of OH (Bhatt et al., 2015). Animals were acclimated to tilt chair procedures for a minimum of 3 months prior to baseline. The tilt chair apparatus was designed to alternately position the conscious monkey between horizontal (supine in a seated position) and vertical (90° head-up) positions. The tilt procedure was conducted as previously described (Bhatt et al., 2015). Briefly, the monkey was positioned horizontally (supine) for ~10 min to achieve a stable hemodynamic baseline, followed by a 90° (head-up) vertical position for ~3 min, then a horizontal position. Systolic BP (SBP) and HR were continuously monitored during the procedure.

Two consecutive tilts (separated by 10 min) were performed in each session. If required, a third tilt was added to further characterize the response. Each tilt was analyzed separately. Changes in SBP and HR from supine levels at 2 and/or 3 min (10-s average) posthead-up tilt were used to assess differences in mean values between the tanezumab-treated group and the control group. The clinical definition for OH, defined as a decrease ≥20 mmHg in SBP from the supine value at 2 and/or 3 min posthead-up tilt, was applied (Freeman et al., 2011). Tilt assessments were undertaken twice prestudy (baseline) and
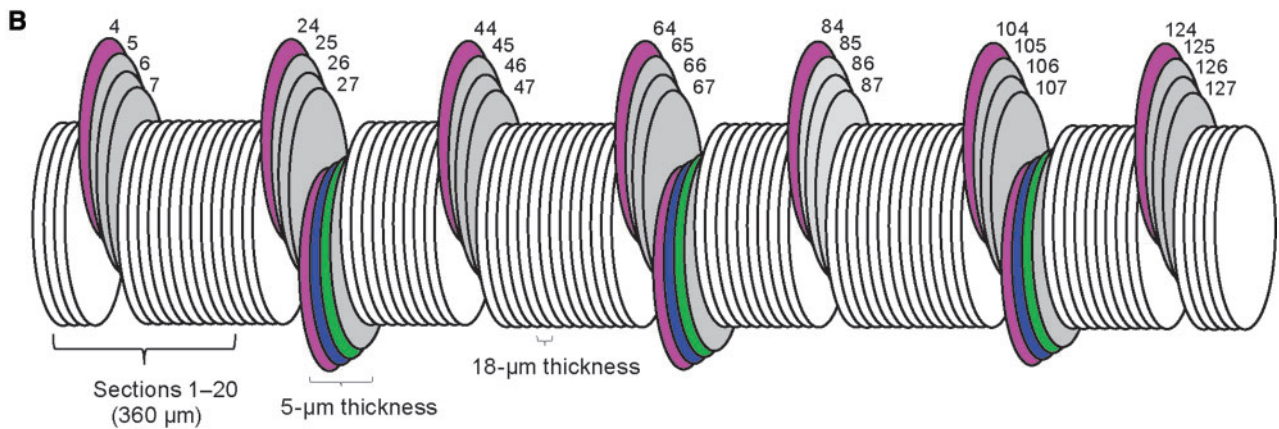
Figure 2. Schematic representation of tissue sectioning and staining for the assessment of neuronal cell death, morphology, and stereology in sympathetic ganglia of nonhuman primates in (A) study 1 and (B) study 2. H&E, hematoxylin, and eosin; TUNEL, terminal deoxinuclotidyl transferase dUTP nick end labeling.

Table 1. Neurohistopathology Assessments in Studies 1 and 2

Tissue	Morphology H&E	Necrosis Fluoro-Jade B	Apoptosis (TUNEL)	Stereology (neuron size, counts, and ganglion volume)	TEM
Study 1[a]					
CTG	×	×	×	×	NE
SCG	×	×	×	×	NE
Study 2[b]					
CTG	NE	NE	NE	NE	×
SCG	×	×	×	×[c]	NE

[a]Assessments performed at 3 months, 6 months and at the end of the recovery period.
[b]Assessments performed at 48 h, 1 week, 2 weeks and 1 month.
[c]Assessment performed at 1-month time point only.
CTG, cervicothoracic ganglia; H&E, hematoxylin and eosin; SCG, superior cervical ganglion; TEM, transmission electron microscopy; TUNEL, terminal deoxinuclotidyl transferase dUTP nick end labeling; NE, not evaluated.
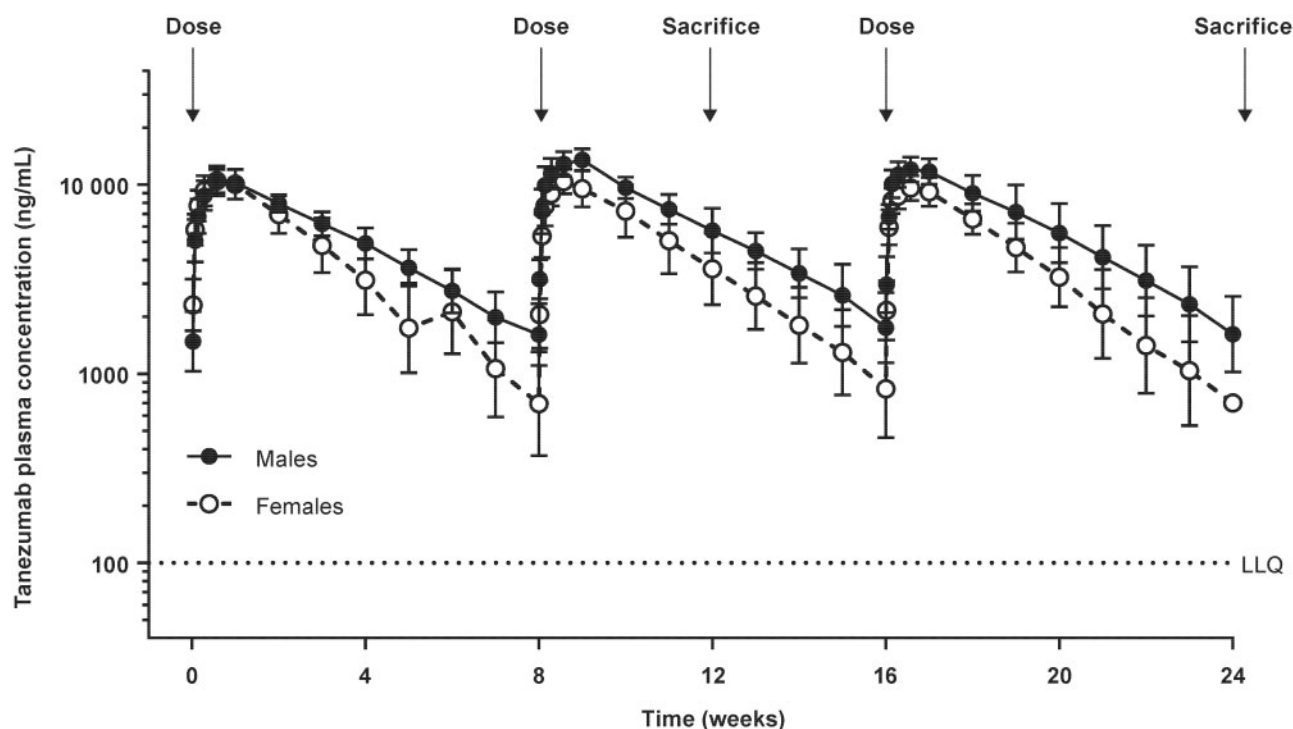

Figure 3. Mean tanezumab plasma concentration (standard deviation) vs time in male and female monkeys administered tanezumab 1.2 mg/kg/Q8W SC once every 8 weeks and sacrificed on study week 12 (3-month cohort) and week 24 (6-month cohort) in study 1. LLQ, lower limit of quantitation for tanezumab bioanalytical assay.

every 2 weeks during the treatment and nondosing recovery phases (Figure 1C).

Statistical analysis. Statistical analyses for stereology data used a 2-tailed, independent *t*-test conducted separately for each sex. Statistical analyses were performed between dose groups against their respective (same euthanasia time) control groups. A P-value of <.05 was considered to be statistically significant. SBP and HR data were analyzed using a repeated-measure analysis of covariance (ANCOVA) using the second baseline measurement as a covariate. Sexes were combined and comparisons to vehicle were made for each dose.

RESULTS

Exposure and ADA Analyses
In study 1, SC dosing of tanezumab 1.2 mg/kg/Q8W resulted in slightly higher tanezumab plasma concentrations in male vs

female monkeys (Figure 3). The TK data confirmed the exposure predictions in the 6-month study with exposures 5.9× (males) and 3.8× (females) the clinical exposure (10 mg SC) based on the mean C_{ave} of the third and last dose administered. Based on the mean C_{max} of the third and last dose administered, the exposure margin over the 10-mg SC clinical dose was 9.1× and 6.5× in males and females, respectively.

In study 2, C_{ave} and C_{max} over the 4-week duration of the study for the males were 8× and 12×, respectively, what was observed on average for the clinical dose of 10 mg SC/Q8W.

In study 3, C_{ave} and C_{max} after the last dose of 1.2 mg/kg over the 8-week dosing interval were approximately 3× and 5×, respectively, what was observed on average at the clinical dose of 10 mg SC/Q8W, while C_{ave} and C_{max} at 30 mg/kg were approximately 900× and 700×, respectively, the clinical exposure.

In study 1, several monkeys developed ADA (n = 29 out of 52) and many had compromised exposure to tanezumab. Monkeys with compromised exposure were replaced by spare monkeys so that all animals evaluated at termination had adequate exposure.
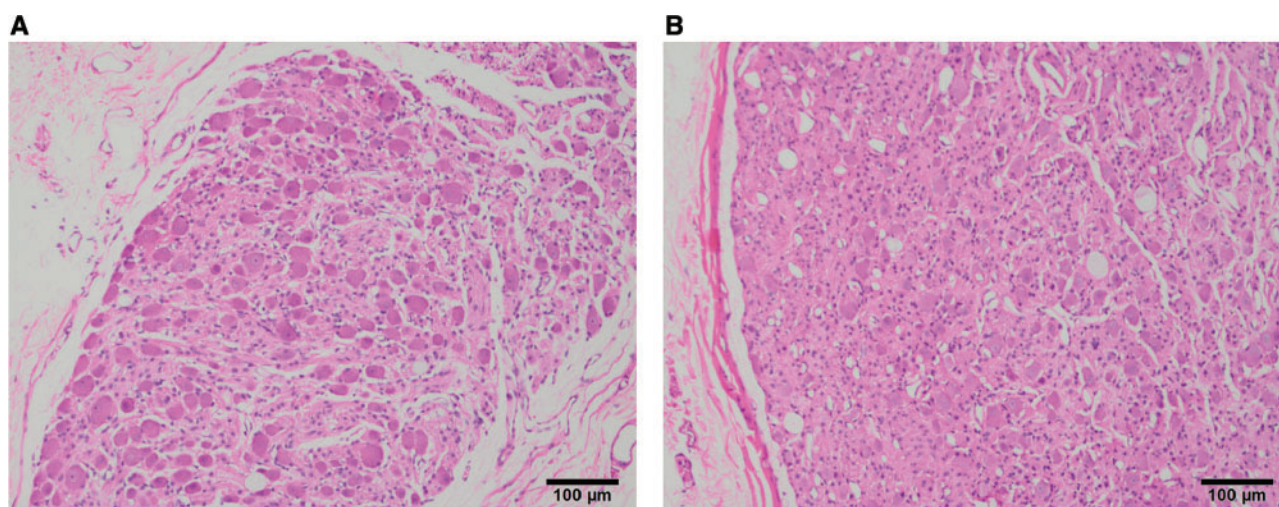
Figure 4. Superior cervical ganglion, paraffin embedded, H&E stained 5-μm sections from (A) control and (B) 1.2 mg/kg tanezumab treated monkeys. H&E, hematoxylin, and eosin.

Table 2. Evaluation of Neuronal Cell Death in Studies 1 and 2

	Presence of Cell Death/Timing of Evaluation					
Staining	48 Hours	1 Week	2 Week	1 Month	3 Month	6 Month
Hematoxylin and eosin	None	None	None	None	None	None
Fluoro-Jade B	None	None	None	None	None	None
TUNEL	None	None	None	None	None	None
TEM	None	None	None	None	NA	NA

TUNEL, terminal deoxinuclotidyl transferase dUTP nick end labeling, TEM, transmission electron microscopy; NA, not applicable.

In study 2, 3 monkeys developed ADA and while the individual exposures of the ADA-impacted animals were lower than their ADA-negative counterparts, mean overall exposure was not significantly affected.

In study 3, 4 monkeys (3 females, 1 male) treated with tanezumab 1.2 mg/kg/Q8W had lower exposure compared to ADA-negative animals on days 57 and 113 due to ADA. The ADA-positive animals were not replaced and remained on study despite lower exposure to tanezumab compared to ADA-negative monkeys (due to logistic difficulties in having radiotelemetry spare animals). The inclusion of these 4 monkeys in the low-dose (1.2 mg/kg/Q8W) group had no impact on the objective of the study because a second, high-dose group (30 mg/kg/week) was included. No animals in the 30 mg/kg/week group tested ADA-positive.

Neurohistopathology
Sympathetic ganglia were examined using a comprehensive, systematic sectioning scheme (every 360 μm through the ganglion) using multiple staining methodologies designed to provide a detailed morphologic evaluation with increased sensitivity towards the detection of necrotic/apoptotic neurons. Approximately 9000–12 000 neurons per ganglion were evaluated for evidence of neuronal cell death at the 3-month, 6-month, and recovery time points in study 1 and ~10 000 neurons per SCG ganglion were evaluated at the 48-h, 1 week, 2 weeks, and 1 month time points in study 2. This extensive examination did not reveal any evidence of neuronal cell death in either the SCG or CTG of any animal administered either vehicle control or tanezumab, at any time point (Table 2).

Morphologic evaluations by light microscopy of the SCG revealed 2 changes related to tanezumab administration: *Neurons, small, diffuse* (meaning neurons that were smaller than controls located diffusely throughout the ganglia; a change referred to as neuronal atrophy in some publications (Angeletti et al., 1971; Ruit et al., 1990) and *glial cells, increased density, diffuse* in males and females at various time points (Table 3). H&E and toluidine blue staining revealed generally smaller neurons in cross-section area and the overall cellularity of the glial cells appears increased (likely due to the decreased size of the neurons) with tanezumab treatment. This subtle change, verified at the stereologic evaluation, was recorded as neuronal atrophy (Figure 4; Supplementary Figs. 3 and 4). Satellite glial cells and Schwann cells are the primary glial cells in ganglia. This increased density of glia was not localized within the ganglia, but was diffusely distributed throughout. Morphologic results of the CTG were consistent with those from SCG. The increased glial cell density did not represent gliosis; there was no evidence of enlarged/activated glial cells or glial cell proliferation (such as mitotic activity). Rather, the increased glial cell density was likely due to the decrease in neuronal size resulting in the visual appearance of glial cells occupying more of the ganglion space.

Stereologic Evaluations
Ganglion volume. When compared to control monkeys, mean SCG ganglion volume was significantly lower (−34%, $P = .0259$) in male, but not female, monkeys after 3 months of tanezumab treatment (Figure 5). Tanezumab treatment did not affect mean ganglion volume in either sex at the 1- and 6-month time points, as well as at the end of the recovery period. The effects observed after

Table 3. Key Morphological Observations in the Superior Cervical Ganglion of Male and Female Monkeys Administered Tanezumab SC 1.2 mg/kg/Q8W

SCG: Light Microscopy	48 Hours	1 Week	2 Week	1 Month	3 Month	6 Month	6 Months Plus Recovery
Neurons, small, diffuse, males							
Incidence	1/6	1/6	6/6[b]	6/6[b]	6/7[b]	4/6[b]	0/6
Average severity[a]	0.17	0.33	2.00[b]	2.67[b]	1.86[b]	1.00[b]	0.00
Neurons, small, diffuse, females							
Incidence	NA	NA	NA	NA	3/5[b]	2/5	0/4
Average severity[a]	NA	NA	NA	NA	1.00[b]	0.40	0.00
Glial cells, increased density, diffuse, males							
Incidence	1/6	1/6	6/6[b]	6/6[b]	6/7[b]	4/6[b]	1/6
Average severity[a]	0.17	0.33	2.00[b]	2.67[b]	1.71[b]	1.00[b]	0.17
Glial cells, increased density, diffuse, females							
Incidence	NA	NA	NA	NA	3/5[b]	2/5[b]	0/4
Average severity[a]	NA	NA	NA	NA	1.40[b]	0.60[b]	0.00

[a]Severity scale: 1 = slight; 2 = minimal; 3 = mild; 4 = moderate; 5 = severe.
[b]Tanezumab-related effect.
NA, not applicable; Q8W, every 8 weeks; SCG, superior cervical ganglia; SC, subcutaneous.

3 months of tanezumab treatment did not progress or persist over time despite continued exposure to tanezumab and were fully reversible upon withdrawal of tanezumab treatment.

Neuron size/area. Tanezumab treatment resulted in a shift toward smaller neurons with a significantly lower (−18 to −34%) mean average neuron size/area in the SCG when compared to vehicle treatment ($P \leq .0214$; Figure 6). These effects were present in males at 1, 3, and 6 months, whereas the effects in females were observed only at the 6-month time point. This effect was not present at the end of the recovery period in either males or females. The mean average neuron size/area observed after 1 month of tanezumab treatment did not decrease further over time despite continued exposure and was fully reversible upon withdrawal of tanezumab.

Total estimated neuron count. When compared to vehicle-treated controls, mean estimated total neuron counts in the SCG ganglion were significantly lower (−33% to −38%) in male monkeys treated with tanezumab for 1 month and for 3 months ($P \leq .0093$; Figure 7). There was no effect of tanezumab on mean estimated total neuron counts in males following treatment for 6 months or at the end of the recovery period.

In females, mean estimated total neuron counts were lower (−37%) following tanezumab treatment for 3 months ($P = .0281$). No effects were observed in females after 6 months of treatment or at the end of the recovery period. The mean estimated total neuron counts observed after 1 and 3 months of treatment in the males, and 3 months of treatment in the females, did not decrease further over time despite continued exposure to tanezumab and were fully reversible upon withdrawal of treatment. Reversal, combined with a lack of evidence of neuronal necrosis/apoptosis, indicated the lower neuron counts were due to under-recognition of neurons (during stereology evaluation), not to any actual loss of neurons.

Transmission electron microscopy. Results from the TEM evaluation were consistent with those from the morphologic evaluations by light microscopy, with no evidence of cell death (including no evidence of neuronal cell death), phagocytosis, or inflammation (Table 3). Smaller neurons were observed only at the 1-month time point and were characterized by condensed cytoplasm (ie, all organelles were present but were generally within a cytoplasm compartment that appeared small/condensed).

No tanezumab-related effects were identified at the earlier time points.

Cardiovascular evaluation (study 3). Tanezumab (1.2 mg/kg/Q8W or 30 mg/kg/week) did not have any effects on ambulatory SBP (Figs. 8A and B), HR or 24-h activity (data not shown) when compared to time-matched vehicle controls. Furthermore, no significant effects were observed on the group mean SBP responses to the tilt-chair challenge conducted during the study (Figs. 8C and D). The mean responses in tanezumab treated groups were typical, and similar to vehicle, as evidenced by a transient decrease in BP induced by the head-up tilt, which returned to pretilt (supine) levels within 20–30 s (Figure 8C) (Bhatt et al., 2015). Isolated incidences of OH were observed during the 6-month treatment phase (Table 4) and are detailed below.

In the vehicle control group, no OH responses were observed. One female exhibited sporadic decreases in SBP that exceeded 20 mmHg during the second tilt on day 116. However, the mean decrease of 18 mmHg in SBP at 3 min post-tilt did not meet the OH definition criteria of the study. This animal showed normal tilt responses at the subsequent tilt on day 129 and throughout the remainder of the study.

In the tanezumab low-dose group (1.2 mg/kg/Q8W), 1 female exhibited an OH response on the second tilt on day 73, as evidenced by a decrease in SBP of ∼50 mmHg at 2 and 3 min posthead-up tilt, with a third tilt confirming the OH response. This animal showed an improvement (SBP decreases <20 mmHg at 2–3 min posthead-up tilt) on subsequent assessment performed on day 87, with a normal tilt response at the next tilt undertaken on day 101 and throughout the remainder of the study.

In the tanezumab 30 mg/kg dose group, 1 male exhibited an OH response on day 142. An OH response was again observed on the subsequent assessment on day 156 (last assessment of the dosing phase), with responses to the second and third tilts on day 156 exhibiting decreases in SBP of 29–40 mmHg at 2 and 3 min posthead-up tilt. During the 2-month nondosing recovery phase, progressive improvement in the tilt profile of this animal was observed with full recovery, as evidenced by normal SBP tilt response, observed during the last month of the recovery phase. Measured tanezumab exposures for this animal in the last month of the study were 45.1 μg/ml (day 197) and 19.7 μg/ml (day 211) at the time of the last tilt session. This corresponds to approximately 45- and 20-fold higher than the C_{ave} seen with a clinical dose of 10 mg SC, respectively.
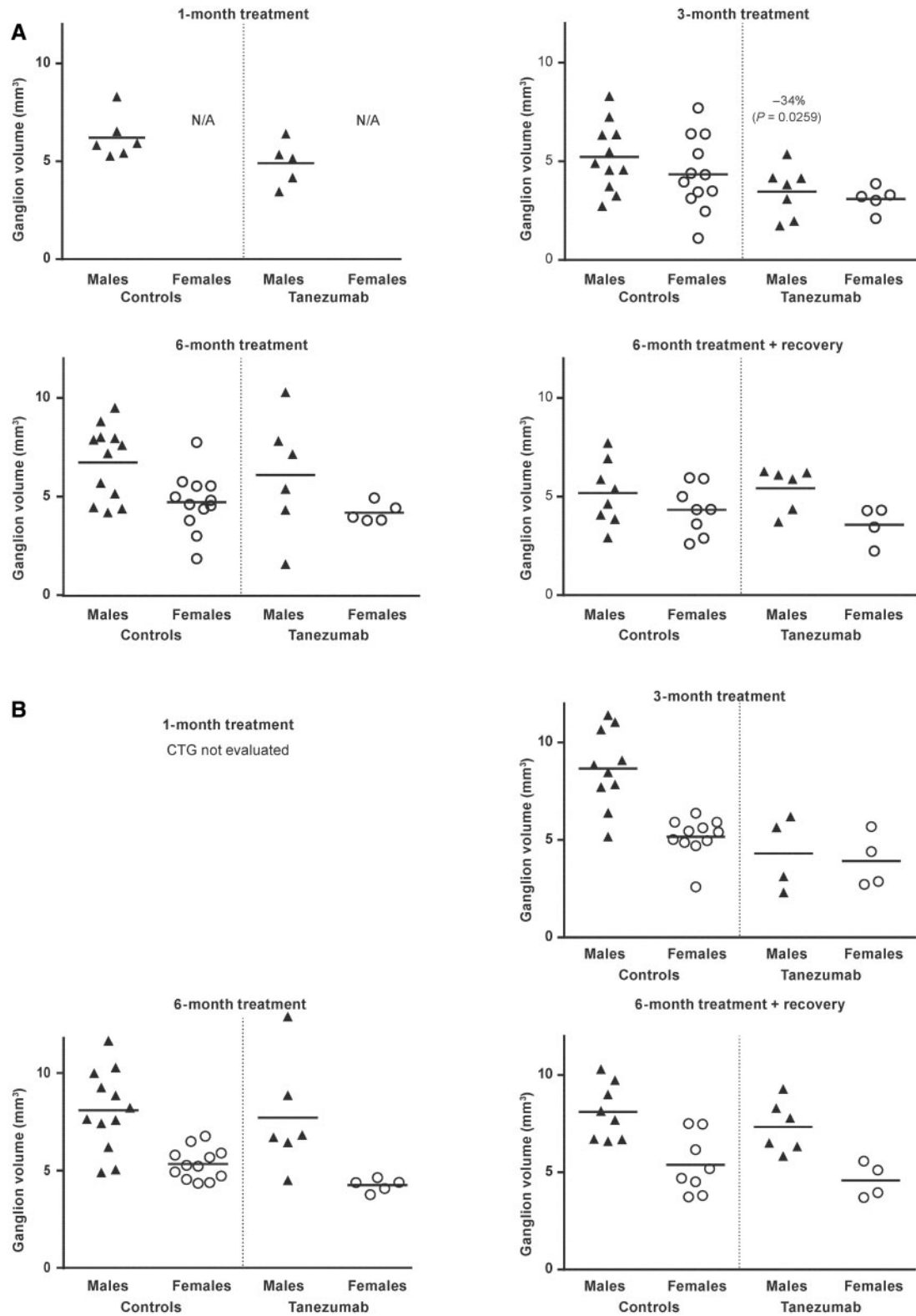
Figure 5. Individual and group mean (A) superior cervical ganglion volume and (B) cervicothoracic ganglion volume in monkeys administered vehicle (controls) or tanezumab at 1.2 mg/kg/Q8W. Q8W, every 8 weeks; CTG, cervicothoracic ganglion; N/A, not applicable.

DISCUSSION

These studies indicate that NGF inhibition by tanezumab, at levels sufficient to result in clinically meaningful reduction in pain scores, does not result in sympathetic neuronal cell death nor observable changes in sympathetic function. This is supported by the lack of observation of dying cells at any time and
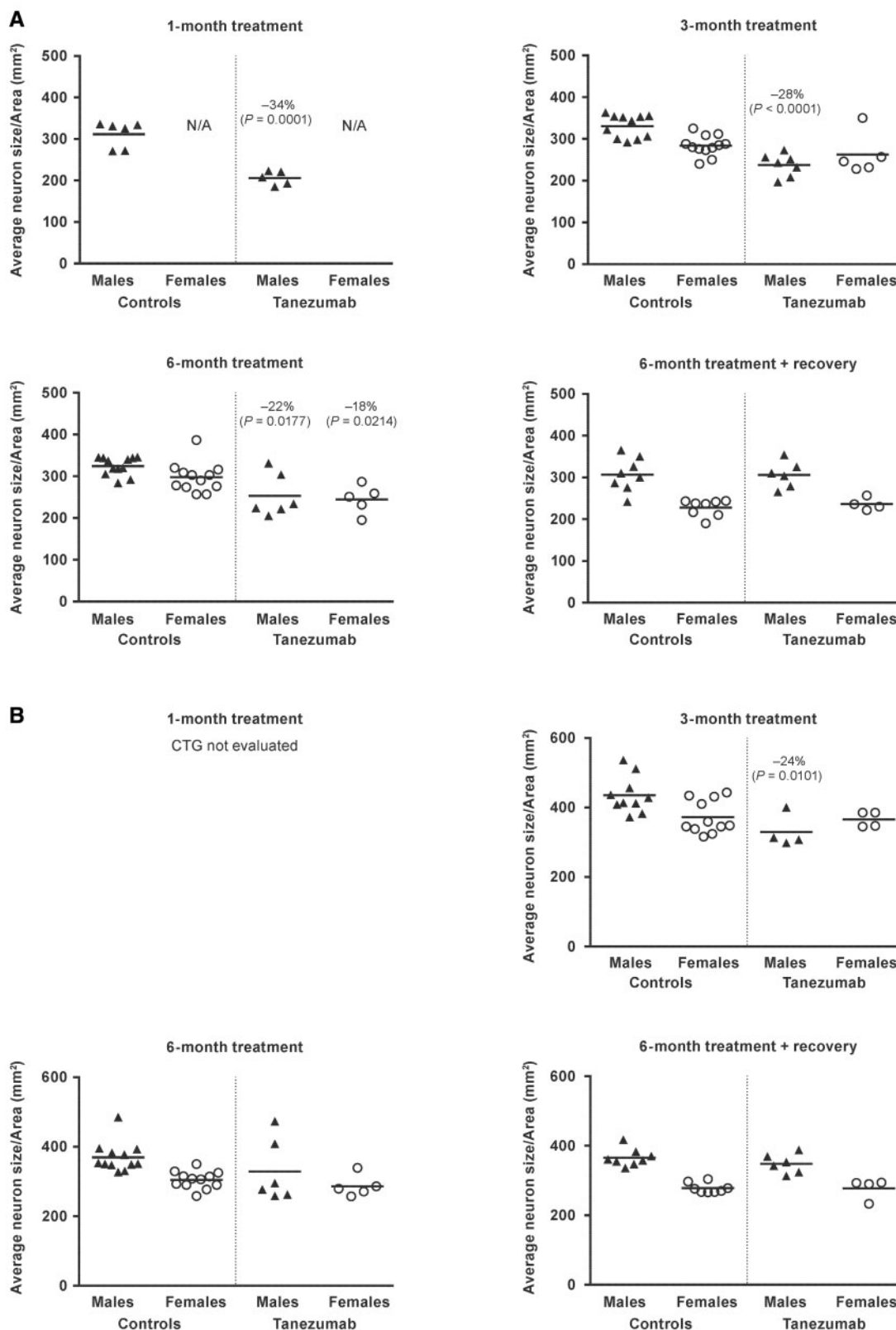
Figure 6. Individual and group mean average neuron size/area in the (A) superior cervical ganglion and (B) cervicothoracic ganglion in monkeys administered vehicle (controls) or tanezumab at 1.2 mg/kg/Q8W. Q8W, every 8 weeks; CTG, cervicothoracic ganglion; N/A, not applicable.
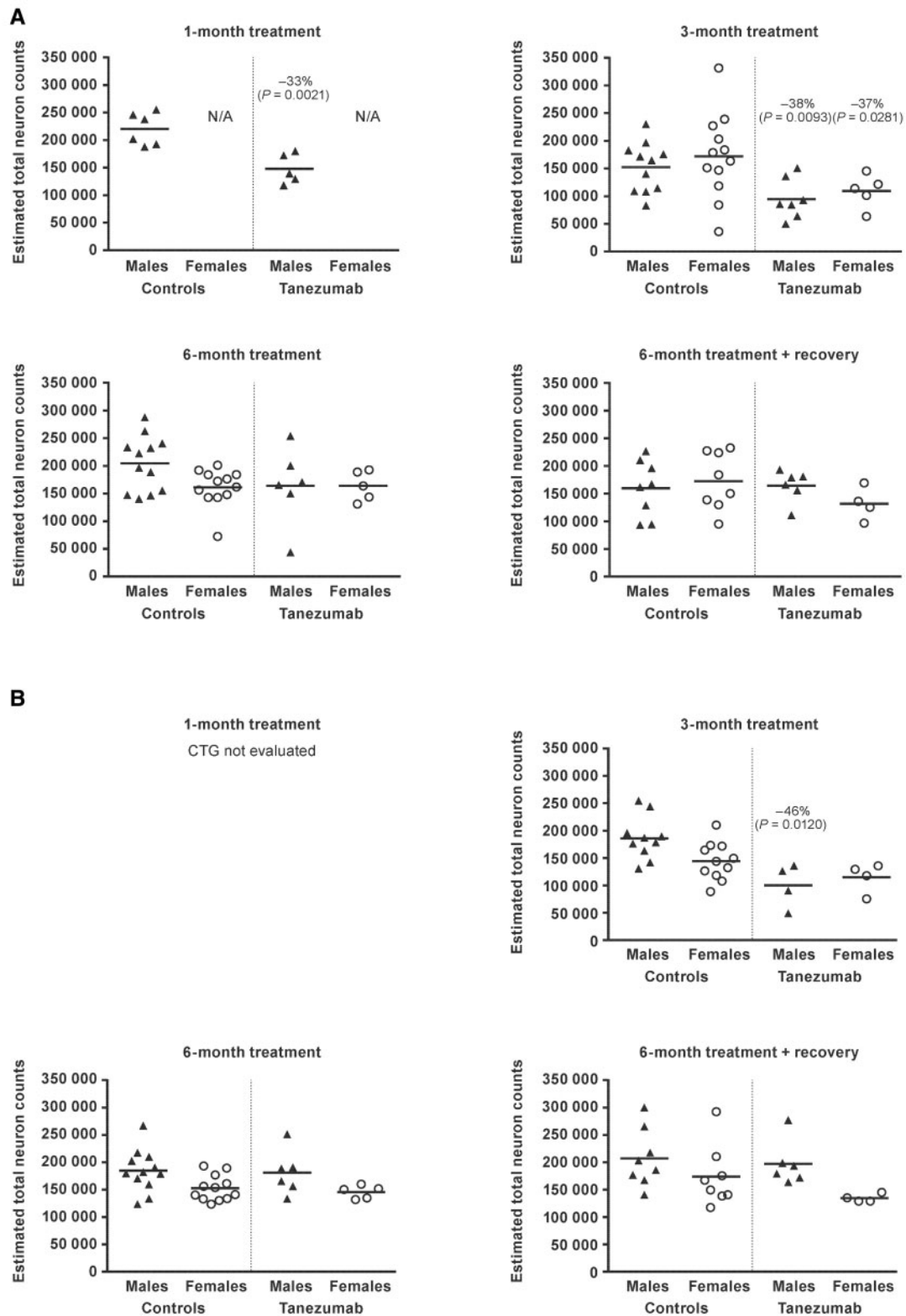
Figure 7. Individual and group estimated total neuron counts in the (A) superior cervical ganglion and (B) cervicothoracic ganglion in monkeys administered vehicle (controls) or tanezumab at 1.2 mg/kg/Q8W. CTG, cervicothoracic ganglion; Q8W, every 8 weeks; N/A, not applicable.

complete recovery of neuronal cell counts upon treatment cessation. Morphologic changes occurred during this treatment regimen, but they did not progress and were not reflected in any detected functional changes in sympathetically mediated events. These

results agree with results from clinical studies of tanezumab indicating no evidence of sympathetic dysfunction (Brown et al., 2015).

Animals in the current studies were exposed to significantly higher tanezumab levels than those seen in clinical studies to
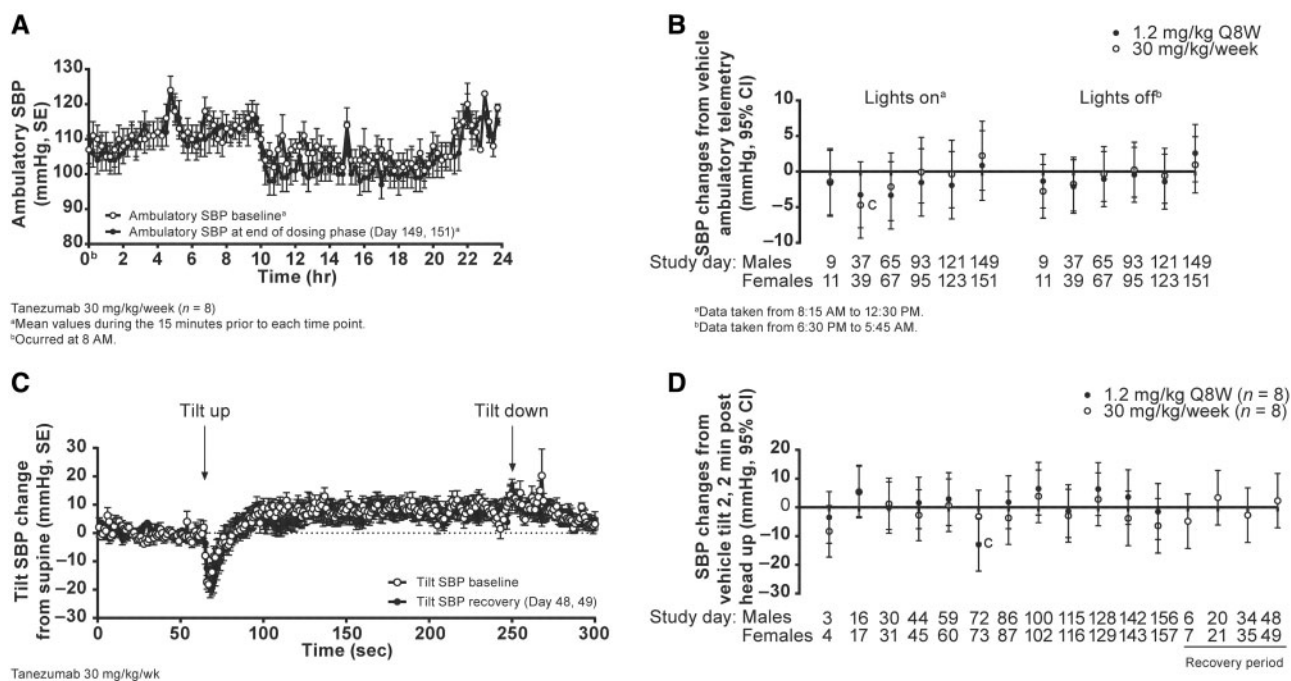
Figure 8. Combined results for male and female monkeys treated with tanezumab: (A) 24-h ambulatory SBP, (B) SBP change from vehicle, (C) tilt change from supine SBP, and (D) SBP change from vehicle. [c]P< .05; CI, confidence interval; Q8W, every 8 weeks; SBP, systolic blood pressure; SE, standard error.

Table 4. Observations of Orthostatic Hypotension in Study 3

Group	Observations of OH[a]	OH Responders[b]
Vehicle	0[c]/96[d]	0/8
Tanezumab 1.2 mg/kg/Q8W	1/96	1/8
Tanezumab 30 mg/kg/week	2/96	1/8

[a]OH was defined as a decrease (from the supine value) in SBP $\geq$20 mmHg at 2 and/or 3 min posthead-up tilt test.

[b]The numerator indicates the number of animals showing at least one OH response during the study. The denominator indicates the total number of animals evaluated in each group.

[c]One vehicle-treated female exhibited a decrease of 18 mmHg in SBP at 3 min post-tilt test on day 116.

[d]Total number of tilt challenge sessions undertaken for each group over the 6-month dosing phase. Each challenge session consisted of two consecutive tilts (separated by 10 min). If required, a third tilt was added to further characterize the observed response.

OH, orthostatic hypotension; Q8W, every 8 weeks; SBP, systolic blood pressure.

date. In studies 1 and 2, females had, on average, 4-fold higher and males had 6-fold higher plasma levels than those providing robust pain relief in clinical trials (Jonsson et al., 2016; Lalovic et al., 2010; Xie et al., 2009). Earlier nonclinical studies (and study 3 herein) used much higher doses of tanezumab (up to 30 mg/kg/week, corresponding to exposure multiples up to ~900-fold that seen in clinical studies utilizing 10 mg SC/Q8W dosing) (Zorbas et al., 2011).

Morphologic evidence of neuronal death is typically transient (Switzer, 2011), making the timing of morphologic observations following drug/biologic exposure critical. In the present studies, tissues from numerous time points were examined in order to eliminate timing as a cause for missing neuronal cell death. A variety of staining methodologies and TEM were also used to improve the sensitivity of the evaluations. No signs of a single dying neuron were observed at any time after treatment

despite examination of several thousand neurons from each ganglion from each animal. If the ~33% lower cell count observed at 1 month in the male animals was real and due to neuronal cell death, the morphologic evaluation would have identified neuronal death. Furthermore, the observed decrease in neuronal counts completely reversed upon treatment cessation. These data strongly indicate neuronal death is not occurring in sympathetic ganglia of adult nonhuman primates following tanezumab exposure. This is consistent with the growing consensus in literature that mature sympathetic neurons become insensitive to NGF deprivation, promoting multiple survival mechanisms to prevent cell death by apoptosis (Kole et al., 2013; Kristiansen and Ham, 2014).

Although there was no evidence of cell death, there were morphologic changes observed in the ganglia of treated animals. Data from morphology and stereology studies were consistent in showing a decrease in neuronal size and an increase in the density of glial cells. The decrease in neuronal size in tanezumab-treated animals is consistent with data from earlier studies using anti-NGF antibodies in rodents (Gorin and Johnson, 1980; Johnson et al., 1982; Otten et al., 1979; Ruberti et al., 2000; Ruit et al., 1990). This change in cell size was especially noted in male animals and seemed to be more notable in the SCG than the CTG. Lower tanezumab exposure in female animals may have contributed to the observed difference in magnitude of the effect on neuronal size between male and female animals. This change in cell size did not progress with treatment duration in the males and was fully reversible after treatment was stopped. In control animals at the 3-month, 6-month, and recovery time points, males showed higher neuron size/area compared with females in both SCG and CTG. A similar difference in average neuron size/area between male and female control monkeys was observed in a study previously conducted with tanezumab (Zorbas et al., 2011). The reason for the observed difference is unknown. There was also evidence of

a decrease in average ganglion volume, although this parameter was highly variable and only reached statistical significance at the 3-month time point in the male cynomolgus monkey SCG.

One interesting observation from morphologic examination of the ganglia was the relatively consistent finding of increased density of glial cells after 2 weeks of treatment. The increased density persisted with a slight decline at 3 and 6 months, and recovered after treatment stopped. This is unlikely to be gliosis because there were no signs of glial activation or cell proliferation. The arrangement of glial cells, notably satellite glial cells, around neurons would be visualized as an increased cell density in association with neuronal atrophy. Consistent with this, stereologic assessment of the CTG (ganglia from controls and ganglia with evident increased glial cell density) in a prior study in nonhuman primates (unpublished data) showed no increase in overall (absolute) total glial number following tanezumab exposure.

The weight of evidence from these studies (notably the return of neuron counts to control levels given a sufficient treatment-free period) and the lack of definitive neuronal necrosis (such as images of necrotic neurons) in prior published studies by other authors strongly suggest neuron death was not responsible for the decrease in neuron counts observed in quantitative investigations. The unbiased stereologic methods used in these studies further support this. The optical dissector/fractionator was used to sample the ganglia (the three-dimensional reference space) in a systematic random manner (using sections every 360 μm). Counting rules were followed (each neuron was reduced to a small point by using a nucleolus as the counting point) so just a reduction in cell size would not affect cell counts. While other counting points (center of the nucleus, top of the cell, top of the nucleus) may also be used, the nucleolus was considered the most reliable "point" for sections used in this study.

The size reduction in the neurons, the clustering of glial cells around these smaller neurons, and possibly obscured nucleoli (by clustering satellite glial cells that surround neurons in three dimensions, an arrangement preserved in the 18-μm sections used in these studies) all likely resulted in reduced counts because of under-recognition of neurons. It is assumed these same factors affected data presented in prior publications by other authors. When neurons were killed by a test article such as guanethidine, the remaining neurons increased in size after a recovery period (Zahner et al., 2016). Following recovery in the current study, the neuron size/area of tanezumab-treated animals was not larger than control neurons, consistent with neurons not being killed in these studies. TEM of the ganglia did not reveal any obvious changes in neuronal morphology that would result in under-recognition. However, using TEM, neurons are readily identified by morphologic characteristics not visible using light microscopy (eg, association of neurons with surrounding satellite glial cell processes). Previous studies showed a reduced complexity of dendritic arbor (Ruit et al., 1990) and perhaps there are other factors that lead to under-recognition. At least 1 other report postulated that the reduction in neuron size might be responsible for the decreased cell counts, stating "A caveat in interpreting these results [referring to decreased neuron counts] is that, in the presence of severe atrophy it may be difficult to distinguish neurons from non-neuronal cells. Thus, the degree of cell death may be overestimated" (Ruit et al., 1990). We recently showed that using stereology techniques optimized to minimize process-related tissue shrinkage, treatment with an anti-NGF antibody was not associated with a reduction in the number of neurons in the SCG of rats, suggesting that process-related tissue shrinkage may be responsible, at least in part, for the undercounting of neurons in the current studies (Marcek et al., 2016)

In light of these morphologic changes and previously reported biochemical effects of anti-NGF (Bjerre et al., 1975; Goedert et al., 1978), it was of interest to assess the function of the SNS in these animals. Radiotelemetry was used to assess ambulatory cardiovascular parameters and a validated nonclinical correlate of the clinical OH test was used to assess SNS function while undergoing a tilt challenge (Bhatt et al., 2015). In these studies, one cohort of animals was treated the same way as in the morphology studies (approximately 5 times the clinical exposure) and another was dosed at a much higher level giving plasma exposure ∼900 times that achieved in the clinic. Administration of tanezumab had no effect on ambulatory cardiovascular parameters (BP, HR, body temperature and activity) or on group mean changes in SBP following head-up tilt assessed over the 6 months of the study. Isolated incidences of OH were observed in a single monkey in each of the low- and high-dose groups. The OH observed in the low-dose monkey did not repeat on subsequent tilt assessments. The OH observed in the high-dose monkey recovered fully during the 2-month non-dosing recovery period even in the presence of significant circulating plasma levels of tanezumab. One vehicle-treated female exhibited sporadic decreases in SBP that exceeded 20 mmHg during the second tilt on day 116, but when analyzed showed a mean decrease of 10 and 18 mmHg in SBP at 2 and 3 min post-tilt, respectively. These data suggest that tanezumab treatment did not have any major effects on sympathetic function. This finding is consistent with an extensive examination of clinical trial data, which found no increase in adverse events related to SNS function in tanezumab-treated patients (Brown et al., 2015).

Taken together, the data presented here help to clarify previous data and strongly indicate that tanezumab does not cause neuronal cell death in the adult nonhuman primate SNS. Supratherapeutic doses of tanezumab appear to have no progressive or irreversible effects in adult nonhuman primate SNS as measured by morphology, stereology or cardiovascular functional studies.

SUPPLEMENTARY DATA

Supplementary data are available at *Toxicological Sciences* online.

ACKNOWLEDGMENTS

FUNDING

REFERENCES

Angeletti, P. U., Levi-Montalcini, R., and Caramia, F. (1971). Analysis of the effects of the antiserum to the nerve growth factor in adult mice. *Brain Res.* **27**, 343–355.

Bhatt, S., Foote, S., Smith, A., Butler, P., and Steidl-Nichols, J. (2015). A non-human primate model for investigating drug-induced risk of orthostatic hypotension and sympathetic dysfunction: Preclinical correlate to a clinical test. *J. Pharmacol. Toxicol. Methods* **73**, 49–55. 10.1016/j.vascn.2015.03.003.

Bjerre, B., Wiklund, L., and Edwards, D. C. (1975). A study of the de- and regenerative changes in the sympathetic nervous system of the adult mouse after treatment with the antiserum to nerve growth factor. *Brain Res.* **92**, 257–278.

Bowman, C. J., Evans, M., Cummings, T., Oneda, S., Butt, M., Hurst, S., Gremminger, J. L., Shelton, D., Kamperschroer, C., and Zorbas, M. (2015). Developmental toxicity assessment of tanezumab, an anti-nerve growth factor monoclonal antibody, in cynomolgus monkeys (Macaca fascicularis). *Reprod. Toxicol.* **53**, 105–118.

Brown, M., Koltzenburg, M., Nguyen, H., West, C., and Verburg, K. (2015). Tanezumab Does Not Cause Sympathetic Nervous System Dysfunction in Clinical Osteoarthritis Studies, *Neurology* 84:14 (suppl), abstr P3.303.

Bueker, E. D. (1948). Implantation of tumors in the hind limb field of the embryonic chick and the developmental response of the lumbosacral nervous system. *Anat. Rec.* **102**, 369–389.

Butt, M., Evans, M., Bowman, C. J., Cummings, T., Oneda, S., Shelton, D., and Zorbas, M. (2014). Morphologic, stereologic, and morphometric evaluation of the nervous system in young cynomolgus monkeys (Macaca fascicularis) following maternal administration of tanezumab, a monoclonal antibody to nerve growth factor. *Toxicol. Sci.* **142**, 463–476. 10.1093/toxsci/kfu192.

Easton, R. M., Deckwerth, T. L., Parsadanian, A. S., and Johnson, E. M., Jr (1997). Analysis of the mechanism of loss of trophic factor dependence associated with neuronal maturation: A phenotype indistinguishable from Bax deletion. *J. Neurosci.* **17**, 9656–9666.

Freeman, R., Wieling, W., Axelrod, F. B., Benditt, D. G., Benarroch, E., Biaggioni, I., Cheshire, W. P., Chelimsky, T., Cortelli, P., Gibbons, C. H., *et al.* (2011). Consensus statement on the definition of orthostatic hypotension, neurally mediated syncope and the postural tachycardia syndrome. *Clin. Auton. Res.* **21**, 69–72.

Goedert, M., Otten, U., and Thoenen, H. (1978). Biochemical effects of nerve growth factor and its antibody on the vas defferens and the adrenal medulla. *Neurosci. Lett.* **8**, 71–76.

Gorin, P. D., and Johnson, E. M. (1979). Experimental autoimmune model of nerve growth factor deprivation: Effects on developing peripheral sympathetic and sensory neurons. *Proc. Natl. Acad. Sci. U.S.A.* **76**, 5382–5386.

Gorin, P. D., and Johnson, E. M., Jr (1980). Effects of long-term nerve growth factor deprivation on the nervous system of the adult rat: An experimental autoimmune approach. *Brain Res.* **198**, 27–42.

Gundersen, H. J., Jensen, E. B., Kieu, K., and Nielsen, J. (1999). The efficiency of systematic sampling in stereology–reconsidered. *J. Microsc.* **193**, 199–211.

Guyenet, P. G. (2006). The sympathetic control of blood pressure. *Nat. Rev. Neurosci.* **7**, 335–346.

Hefti, F. F., Rosenthal, A., Walicke, P. A., Wyatt, S., Vergara, G., Shelton, D. L., and Davies, A. M. (2006). Novel class of pain drugs based on antagonism of NGF. *Trends Pharmacol. Sci.* **27**, 85–91.

Johnson, E. M., Jr, Gorin, P. D., Osborne, P. A., Rydel, R. E., and Pearson, J. (1982). Effects of autoimmune NGF deprivation in the adult rabbit and offspring. *Brain Res.* **240**, 131–140.

Jonsson, E. N., Xie, R., Marshall, S. F., and Arends, R. H. (2016). Population pharmacokinetics of tanezumab in phase 3 clinical trials for osteoarthritis pain. *Br. J. Clin. Pharmacol.* **81**, 688–699.

Kole, A. J., Annis, R. P., and Deshmukh, M. (2013). Mature neurons: Equipped for survival. *Cell Death Dis.* **4**, e689.

Kristiansen, M., and Ham, J. (2014). Programmed cell death during neuronal development: The sympathetic neuron model. *Cell Death Differ.* **21**, 1025–1035.

Lalovic, B., Xie, R., Marshall, S., Arends, R., and Population, P. K. (2011). *Analysis of Tanezumab Administered to Healthy Volunteers Subcutaneously or Intravenously*, 5–9 November 2010, Atlanta, GA.

Levi-Montalcini, R., and Booker, B. (1960). Destruction of the sympathetic ganglia in mammals by an antiserum to a nerve-growth protein. *Proc. Natl. Acad. Sci. U.S.A.* **46**, 384–391.

Lindsay, R. M. (1988). Nerve growth factors (NGF, BDNF) enhance axonal regeneration but are not required for survival of adult sensory neurons. *J. Neurosci.* **8**, 2394–2405.

Mantyh, P. W., Koltzenburg, M., Mendell, L. M., Tive, L., and Shelton, D. L. (2011). Antagonism of nerve growth factor-TrkA signaling and the relief of pain. *Anesthesiology* **115**, 189–204.

Marcek, J., Okerberg, C., Liu, C. N., Potter, D., Butler, P., Boucher, M., Zorbas, M., Mouton, P., Nyengaard, J. R., and Somps, C. (2016). Anti-NGF monoclonal antibody muMab 911 does not deplete neurons in the superior cervical ganglia of young or old adult rats. *J. Chem. Neuroanat.* **76**, 133–141.

Mouton, P. (2002). *Principles and Practices of Unbiased Stereology: An Introduction for Bioscientists*. The Johns Hopkins University Press, Baltimore, MD.

National Research Council. (1996). *The Guide for the Care and Use of Laboratory Animals*. National Academy Press, Washington, DC.

Orike, N., Thrasivoulou, C., Wrigley, A., and Cowen, T. (2001). Differential regulation of survival and growth in adult sympathetic neurons: An in vitro study of neurotrophin responsiveness. *J. Neurobiol.* **47**, 295–305.

Otten, U., Goedert, M., Schwab, M., and Thibault, J. (1979). Immunization of adult rats against 2.5 S NGF: Effects on the peripheral sympathetic nervous system. *Brain Res.* **176**, 79–90.

Ruberti, F., Capsoni, S., Comparini, A., Di Daniel, E., Franzot, J., Gonfloni, S., Rossi, G., Berardi, N., and Cattaneo, A. (2000). Phenotypic knockout of nerve growth factor in adult transgenic mice reveals severe deficits in basal forebrain cholinergic neurons, cell death in the spleen, and skeletal muscle dystrophy. *J. Neurosci.* **20**, 2589–2601.

Ruit, K. G., Osborne, P. A., Schmidt, R. E., Johnson, E. M., Jr, and Snider, W. D. (1990). Nerve growth factor regulates sympathetic ganglion cell morphology and survival in the adult mouse. *J. Neurosci.* **10**, 2412–2419.

Sanga, P., Katz, N., Polverejan, E., Wang, S., Kelly, K. M., Haeussler, J., and Thipphawong, J. (2013). Efficacy, safety, and tolerability of fulranumab, an anti-nerve growth factor antibody, in the treatment of patients with moderate to severe osteoarthritis pain. *Pain* **154**, 1910–1919.

Schmued, L. C., and Hopkins, K. J. (2000). Fluoro-Jade B: A high affinity fluorescent marker for the localization of neuronal degeneration. *Brain Res.* **874**, 123–130.

Stewart, J. M. (2012). Mechanisms of sympathetic regulation in orthostatic intolerance. *J. Appl. Physiol. (1985)* **113**, 1659–1668.

Switzer, R. C. (2011). Fundamentals of neurotoxicity detection. In *Fundamental neuropathology for pathologists and toxicologists: principles and techniques* (B. Bolon, and M. T. Butt, Eds), pp. 139–159. John Wiley & Sons, Inc., Hoboken, NJ.

Tiseo, P. J., Kivitz, A. J., Ervin, J. E., Ren, H., and Mellis, S. J. (2014). Fasinumab (REGN475), an antibody against nerve growth factor for the treatment of pain: Results from a double-blind, placebo-controlled exploratory study in osteoarthritis of the knee. *Pain* **155**, 1245–1252.

Xie, R., Arends, R., Olson, S., and Marshall, S. (2009). *Preliminary Pharmacokinetic/Pharmacodynamic (PK/PD) Analysis for the Effect of Tanezumab on Overall Daily Pain Score Data in Adults with Moderate-to-Severe Pain due to Osteoarthritis of the Knee*. Available at: http://www.page-meeting.org/pdf_assets/7555-PAGE%20Tanezumab%20poster%20_2009.pdf. Accessed May 15, 2017.

Zahner, M. R., Liu, C. N., Okerberg, C. V., Opsahl, A. C., Bobrowski, W. F., and Somps, C. J. (2016). Neurophysiological assessment of sympathetic cardiovascular activity after loss of postganglionic neurons in the anesthetized rat. *J. Pharmacol. Toxicol. Methods* **80**, 59–67.

Zorbas, M., Hurst, S., Shelton, D., Evans, M., Finco, D., and Butt, M. (2011). A multiple-dose toxicity study of tanezumab in cynomolgus monkeys. *Regul. Toxicol. Pharmacol.* **59**, 334–342.